Remarkable statistical behavior for truncated Burgers–Hopf dynamics

Andrew J. Majda* and Ilya Timofeyev

Courant Institute of Mathematical Sciences, New York University, New York, NY 10012

A simplified one-dimensional model system is introduced and studied here that exhibits intrinsic chaos with many degrees of freedom as well as increased predictability and slower decay of correlations for the large-scale features of the system. These are important features in common with vastly more complex problems involving climate modeling or molecular biological systems. This model is a suitable approximation of the Burgers–Hopf equation involving Galerkin projection on Fourier modes. The model has a detailed mathematical structure that leads to a well-defined equilibrium statistical theory as well as a simple scaling theory for correlations. The numerical evidence presented here strongly supports the behavior predicted from these statistical theories. Unlike the celebrated dissipative and dispersive approximations of the Burgers–Hopf equation, which exhibit exactly solvable and/or completely integrable behavior, these model approximations have strong intrinsic chaos with ergodic behavior.

One challenging common feature of several important problems in contemporary science, ranging from short-term climate prediction for coupled atmosphere–ocean systems (1–3) to simulating protein folding through molecular dynamics (4, 5), is the important fact that larger-scale features have longer correlation times and are more predictable than the general smaller-scale and shorter time-scale features of these systems with a huge number of degrees of freedom. For these intuitive reasons, for example, many features of climate are much more predictable than the weather at a fixed location. Such circumstances naturally suggest the development of suitable stochastic modeling procedures for reduced systems involving only degrees of freedom with longer correlation times. Systematic mathematical strategies to treat such issues have been developed very recently in different contexts (refs. 4 and 6; A.M., I.T. & E. Vanden Eijnden, unpublished work). The goal of this paper is to introduce and study the simplest one-dimensional system of equations with such features as a highly simplified model for such behavior. Straightforward numerical experiments with this deterministic system, presented below, establish that it has intrinsic stochastic dynamics with many degrees of freedom and longer correlation times on larger scales, with general features that can be predicted *a priori* through simple mathematical arguments and scaling theories. Thus, this model provides a simple unambiguous test problem for stochastic modeling strategies for treating unresolved degrees of freedom.

The model introduced and studied here is the Galerkin truncated spectral approximation to the Hopf or inviscid Burgers equation,

$$u_t + \frac{1}{2}(u^2)_x = 0 . \qquad [1]$$

Various approximations to the Eq. **1** have a long history. With various dissipative terms added to the right-hand side, this equation becomes a model for both shock dynamics (7) and turbulence theory (8) that can be solved exactly (9) with extremely predictable behavior associated with shock formation and propagation. For suitable dispersive terms added to Eq. **1**, the equations become completely integrable once again with

highly predictable and recurrent behavior (7, 10). Goodman and Lax (11) have shown that the simplest naive dispersive difference approximation to Eq. **1** has completely integrable behavior for suitable initial data. In contrast, the approximation to Eq. **1** introduced here has intrinsic stochastic dynamics with strong numerical evidence for ergodicity and mixing as well as scaling behavior, so that the larger scales are more predictable with longer correlation times.

The Model

To develop the approximation to Eq. **1** that defines this model, let $P_\Lambda f = f_\Lambda$ denote the finite Fourier series truncation of f,

$$P_\Lambda f = f_\Lambda = \sum_{|k| \leq \Lambda} \hat{f}_k e^{ikx} . \qquad [2]$$

Here and elsewhere in the paper, it is tacitly assumed that f is 2π periodic and real valued so that complex Fourier coefficients $\hat{f}_k$ satisfy $\hat{f}_{-k} = \hat{f}_k^*$. The positive integer, Λ, from Eq. **2** defines the number of complex valued degrees of freedom in the approximation. With these preliminaries, the model introduced and studied here is the approximation to Eq. **1**,

$$(u_\Lambda)_t + \frac{1}{2} P_\Lambda (u_\Lambda^2)_x = 0 . \qquad [3]$$

This is a Galerkin truncated approximation to Eq. **1**. With the expansion

$$u_\Lambda(t) = \sum_{|k| \leq \Lambda} u_k(t) e^{ikx} , \qquad u_{-k} = u_k^* , \qquad [4]$$

Eq. **3** can be written equivalently as the following system of nonlinear ordinary differential equations for amplitudes $u_k(t)$ with $|k| \leq \Lambda$,

$$\frac{d}{dt} u_k = -\frac{ik}{2} \sum_{\substack{k+p+q=0 \\ |p|,|q| \leq \Lambda}} u_p^* u_q^* . \qquad [5]$$

It is elementary to show that solutions of the either Eq. **3** or Eq. **5** have conservation of both momentum and energy, i.e.,

$$M = \frac{1}{2\pi} \int_0^{2\pi} u_\Lambda(t) = u_0(t) \qquad [6]$$

and

$$E = \frac{1}{4\pi} \int u_\Lambda^2 dx = \frac{1}{2} |u_0|^2 + \sum_{k=1}^{\Lambda} |u_k|^2 \qquad [7]$$

are constant in time for solutions of Eq. 3 or Eq. 5.

The momentum constraint in Eq. 6 is associated with trivial dynamical behavior, and without loss of generality, we set $M = 0$, so that $u_0(t) = 0$ in the formula for energy, E, in Eq. 7. Also, all of the sums in Eq. 5 involve only k with $1 \leq k \leq \Lambda$. Eq. 3 has the conserved quantities in Eqs. 6 and 7 but it is unclear whether it is a Hamiltonian system.

It is well known that nontrivial smooth solutions of Eq. 1 develop discontinuities in finite time and thus exhibit a transfer of energy from large scales to small scales. For functions with $u_k(t)$ identically zero instantaneously for $k > \Lambda/2$, the approximation in Eq. 3 or Eq. 5 represents this energy transfer exactly; however, once this transfer develops in a general solution of Eq. 3 or Eq. 5, the conservation of energy constraint rapidly redistributes the energy in the smaller scales to the larger-scale modes. This effect is responsible for the intuitive fact that the small-scale modes of the system should decorrelate more rapidly than the large-scale modes.

Equilibrium Statistical Mechanics for the Model

It is natural to utilize the conserved quantity given by the energy, E, in Eq. 7 to define an invariant Gibbs measure for equilibrium statistical mechanics. To be able to do this, the ordinary differential equations in Eq. 5 need to satisfy the Liouville property. For a set of ordinary differential equations, $\vec{w}(t) = \vec{F}(\vec{w})$, the Liouville property requires that $\Sigma \, \partial F_i / \partial w_i = 0$, i.e. $\vec{F}$ is incompressible. As mentioned in the preceding paragraph, the equations in Eq. 5 have individual solutions that exhibit compressible transfer of energy to smaller scales. Nevertheless, the equations in Eq. 5 satisfy the Liouville property for statistical solutions; to see this, because $u_0 = 0$ and $u_{-k} = u_k^*$, the modes $u_k = a_k + ib_k$ with $1 \leq k \leq \Lambda$ are the defining modes for the equations in Eq. 5. The equation for $u_k(t)$ in Eq. 5 can be written in the following form in terms of a_k and b_k,

$$\frac{d}{dt}\begin{pmatrix} a_k \\ b_k \end{pmatrix} = \begin{pmatrix} V_k^1 \\ V_k^2 \end{pmatrix} = \begin{pmatrix} 2k(b_k a_{-2k} + a_k b_{-2k}) \\ -2k(a_k a_{-2k} + b_k b_{-2k}) \end{pmatrix} + \qquad [8]$$

the terms without a_k, b_k.

Because $\partial V_k^1 / \partial a_k + \partial V_k^2 / \partial b_k = 0$ as follows from Eq. 8, the Liouville property is satisfied. With this property, the canonical Gibbs measures

$$G_\beta = C_\beta \mathrm{EXP}\left(-\beta \sum_{k=1}^{\Lambda} |u_k|^2 \right), \quad \beta > 0, \qquad [9]$$

are invariant probability measures for the statistical dynamics of Eq. 3 or Eq. 5. Given a value for the mean energy, $\bar{E}$, from Eq. 7, β is given by

$$\beta = \frac{\Lambda}{\bar{E}}, \text{ with } Var\{a_k\} = Var\{b_k\} = \frac{1}{2\beta}, \qquad [10]$$

where Var denotes variance. The canonical Gibbs ensemble predicts a spectrum with equipartition of energy in all modes according to Eq. 10. We show below that these statistical predictions are satisfied with surprising accuracy for Λ of moderate size or larger.

A Scaling Theory for Temporal Correlations

It is a simple matter to present a scaling theory that predicts that the temporal correlation times of the large-scale modes are longer than those for the small-scale modes. Recall from Eq. 10 that the statistical prediction for energy per mode is $\bar{E}/\Lambda = \beta^{-1}$; because $\bar{E}/\Lambda$ has units length^2/time^2, and the wave number k has units length^{-1}, the predicted eddy turnover time for the kth mode, T_k, is given by

$$T_k = \left(\frac{\Lambda}{\bar{E}}\right)^{1/2} \frac{1}{k} = \frac{\beta^{1/2}}{k}, \quad 1 \leq k \leq \Lambda. \qquad [11]$$

If the physical assumption is made that the kth mode decorrelates on the timescale proportional to the eddy turnover time with a universal constant of proportionality, a simple plausible scaling theory for the dynamics in Eq. 3 or Eq. 5 emerges. Thus, the scaling theory implied by Eq. 11 shows that the larger-scale modes in the system should have longer correlation times than the smaller-scale modes. This basic qualitative fact is always confirmed in the numerical simulations reported below. The exact quantitative agreement of computed correlation times with the predictions of the scaling theory is also reported below.

Invariant Low-Dimensional Subspaces with Exact Dynamics

Virtually all inhomogeneous systems with many degrees of freedom and intrinsic stochastic behavior also possess lower-dimensional invariant sets with nongeneric and atypical dynamic behavior. Here we show how to construct large families of lower-dimensional invariant subspaces for the dynamics in Eq. 3 or Eq. 5.

To build these invariant subspaces for dynamics, pick any positive integer k_* satisfying $2 \leq k_* \leq \Lambda$ and consider the unique integer N with

$$Nk_* \leq \Lambda < (N+1)k_*. \qquad [12]$$

Associated with k_*, we build exact solutions of Eq. 5 with nonzero Fourier coefficients only at $u_{\pm jk_*}$ for $1 \leq j \leq N$, i.e., define $\bar{u}_j$ by

$$\begin{aligned} u_{\pm jk_*} &= \bar{u}_{\pm j}, \quad 1 \leq j \leq N \\ u_k &= 0, \qquad k \neq \pm jk_*. \end{aligned} \qquad [13]$$

Functions with Fourier coefficients satisfying the symmetries in Eq. 13 are not only 2π periodic but are also spatially periodic with the smaller period, $2\pi/k_*$. For elegance in notation, given k_*, we rescale time to the faster timescale $\tau = k_* t$, then a short calculation confirms that the nonzero Fourier coefficients in Eq. 13 satisfy the same dynamical equations in Eq. 5 with $2N$ degrees of freedom that are strictly less than 2Λ degrees of freedom in the general solution of the original system, i.e.,

$$\frac{d}{d\tau} \bar{u}_k = -\frac{ik}{2} \sum_{\substack{k+p+q=0 \\ |p|,|q| \leq \Lambda}} \bar{u}_p^* \bar{u}_q^*, \quad \text{for } |k| \leq N, \qquad [14]$$

with $u_k(t) = 0$ for $k \neq \pm jk_*$.

For k_* with $\Lambda/2 \leq k_* \leq \Lambda$, $N = 1$, and the equations in Eq. 14 trivially yield the time independent steady state,

$$\begin{aligned} u_{k_*} &= u_{k_*}^0, \quad \text{any complex constant} \\ u_k &= 0 \qquad \text{for } k \neq k_*, 1 \leq k \leq \Lambda. \end{aligned} \qquad [15]$$

For k_* with $\Lambda/3 \leq k_* < \Lambda/2$, $N = 2$, and the nonzero Fourier components u_{k_*}, u_{-2k_*} are defined through Eq. 14 with $N = 2$, i.e.,

$$\frac{d}{d\tau}\tilde{u}_1 = -i\tilde{u}_1^*\tilde{u}_{-2}^*$$

$$\frac{d}{d\tau}\tilde{u}_{-2} = i(\tilde{u}_1^*)^2 . \qquad [16]$$

First, note that Eq. **16** has the steady-state solution defined by the higher wave number $\tilde{u}_{-2} = \tilde{u}_{-2}^0$, $\tilde{u}_1 = 0$, which corresponds to the steady state already mentioned in Eq. **15**. Linearized perturbations $\tilde{u}_1'$ about this steady state satisfy the equation

$$\frac{d}{d\tau}\tilde{u}_1' = -i(\tilde{u}_1')^*\tilde{u}_{-2}^0 , \qquad [17]$$

with exponentially growing solution so that these higher wave-number steady states are dynamically unstable to lower wave-number perturbations. This is the simplest example exhibiting the tendency of Eqs. **3** or **5** to also transfer energy to larger scales. In fact, the equations with $N = 2$ are completely integrable, because conservation of energy implies that $|\tilde{u}_1|^2 = E - |\tilde{u}_2|^2$ and differentiating the second equation in Eq. **16** yields

$$\frac{d^2}{d\tau^2}\tilde{u}_{-2} = -2|\tilde{u}_1|^2\tilde{u}_{-2} = -2(E - |\tilde{u}_2|^2)\tilde{u}_{-2} . \qquad [18]$$

Eq. **18** is integrable, so the dynamics for $N = 2$ has regular nonchaotic behavior (12).

For k_* with $\Lambda/4 \leq k_* < \Lambda/3$ so that $N = 3$, the dynamics on this subspace already exhibits a mixture of integrable and chaotic behavior, whereas $N = 4$ has completely stochastic dynamics. These results are presented and discussed elsewhere (13).

Numerical Evidence for Ergodicity and Correlation Scaling

Here, numerical evidence is presented that strongly supports the statistical predictions in Eqs. **9** and **11** regarding the dynamics in Eq. **5**. For all the numerical data presented here, a pseudospectral method of spatial integration combined with fourth-order Runge–Kutta time stepping is utilized for Eq. **5**. One can anticipate from Eq. **9**, which predicts energy equipartition, that in dynamic simulations both the high and low spatial wave numbers are equally important, so increased spatial resolution in the pseudospectral algorithm is needed. Here, this is achieved by increasing the length of the array of the discrete Fourier coefficients by adding zeros for wave numbers k with $\Lambda < k \leq \Lambda_*$ and then performing the discrete Fourier transform to x-space on this bigger array for pseudospectral computations; the choice $\Lambda_* \geq 4\Lambda$ works well in practice and is utilized below. With the small Runge–Kutta time step, $\Delta t = 2.5 \times 10^{-4}$, the algorithm conserves the energy from Eq. **7** within $10^{-4}\%$, a relative error of 10^{-6}, for all of the simulations presented here.

The Transition from Deterministic to Stochastic Behavior

First, results are presented for discretization of the deterministic initial data for Eq. **1** given by $u_0 = 2 \sin x$. The exact solution of Eq. **1** remains smooth for t with $t < 0.5$ until a discontinuity forms at $t = 0.5$. Next, the discrete solution of Eq. **5** will be presented for $\Lambda = 50$. The statistical prediction from Eqs. **9** and **10** is striking; the solution of Eq. **5** eventually should achieve statistical equipartition of energy among all modes with variance predicted by Eq. **10** with $\beta = 50$.

The numerical solution exhibits three phases depicted in the snapshots of the solution in Fig. 1 at times $t = 0.4, 0.56, 1.56,$ and 20. The smooth regime occurs for $t < 0.5$, as is evident in the first snapshot from Fig. 1. Beyond the classical breaking time, $t = 0.5$, the solution first develops weak oscillations that increase in character as time evolves. In the second phase of the dynamics, oscillations build up first on small spatial scales and later on
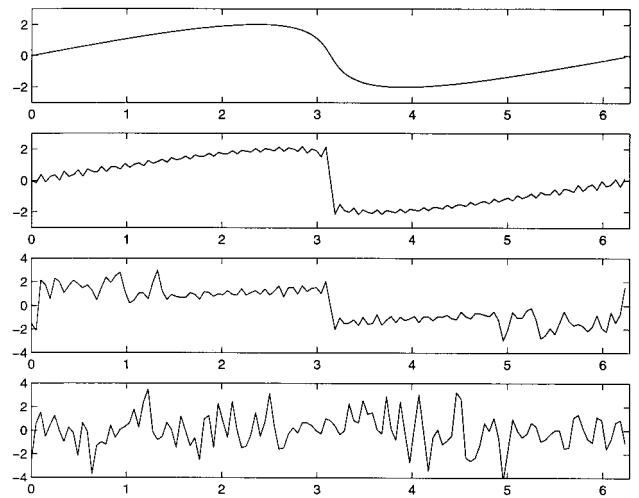

Fig. 1. Solution at time $t = 0.4, 0.56, 1.56,$ and 20.

intermediate spatial scales with memory of the large-scale structure from mode $k = 1$, as is evident from the snapshots at $t = 0.56$ and 1.56 in Fig. 1. In the third phase, all memory of the initial data is lost for the solution, as occurs in the last snapshot at $t = 20$ in Fig. 1.

The graphs of the complex amplitudes of the Fourier modes, $k = 1, 5, 10,$ and 20, depicted in Fig. 2 for the time interval $0 \leq t \leq 40$, confirm the tendency in the second and third phases mentioned above. Clearly by time $t = 40$, the amplitude of the wave number $k = 1$ is completely eroded, and the other modes exhibit random behavior.

Next, it is demonstrated that the solution of Eq. **5** beyond the time $t = 50$ is completely statistical with the equipartition of energy spectrum predicted by Eq. **9** with $\beta = 50$. To measure this, here and elsewhere in the paper, time averaging of an individual solution is performed; thus, the energy in the kth mode is computed by

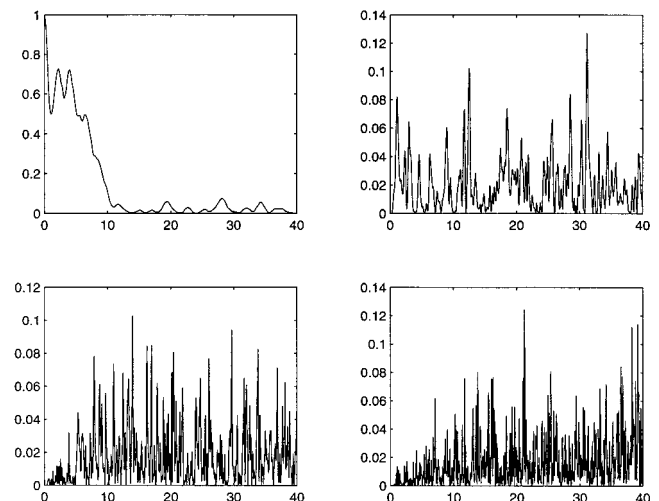$$\langle |u_k|^2 \rangle = \frac{1}{T}\int_{T_0}^{T+T_0} |u_k(t)|^2 dt . \qquad [19]$$

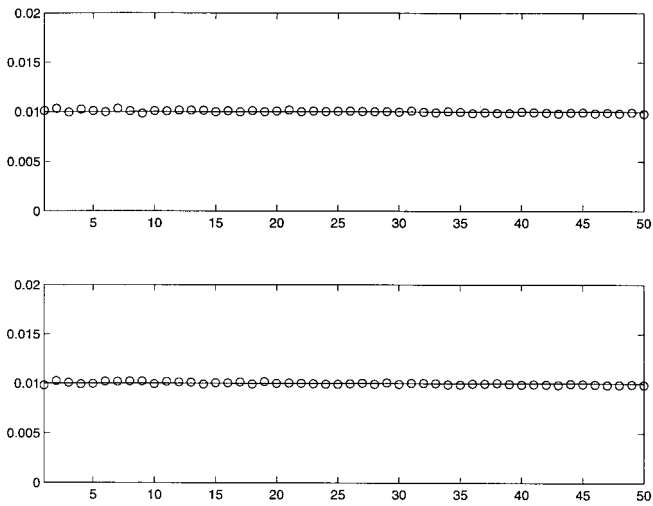**Fig. 2.** Time evolution of the amplitudes of the Fourier coefficients for $k = 1, 5, 10,$ and 20.

Fig. 3. Energy spectrum. Circles, DNS; solid line, canonical predictions.

Fig. 5. Correlation times. Circles, DNS; solid line, predictions of the scaling theory.

For the present simulation, the initial averaging value, $T_0 = 50$, and averaging window, $T = 5,000$, are utilized. This is a severe test because only the microcanonical statistics for an individual solution of Eq. **5** are utilized rather than a Monte-Carlo average over many random initial data as given by the canonical Gibbs ensemble in Eq. **9**.

The energy spectrum for the real and imaginary parts of the Fourier modes is presented in Fig. 3. The straight lines in Fig. 3 correspond to the theoretically predicted value $Var\{\mathrm{Re}u_k\} = Var\{\mathrm{Im}u_k\} = 0.01$, with $\beta = 50$. Clearly, there is statistical equipartition of energy for times t with $t \geq 50$ in the solution of Eq. **5**; the relative errors mostly occur at large scales and do not exceed 4%.

The time correlations $\langle \mathrm{Re}u_k(t + \tau)\mathrm{Re}u_k(\tau) \rangle$ are computed by the same numerical averaging procedure from Eq. **19**. The range in timescales of correlations in the individual Fourier modes varies over 1.5 decades for the value $\beta = 50$ in the present simulation. Fig. 4 depicts the correlation functions of $\mathrm{Re}u_k$ for $k = 1, 2, 3, 10, 15, 20$, illustrating this wide range of timescales present in the system.

The elementary scaling theory for correlation times developed in Eq. **11** is compared with the numerically computed correlation
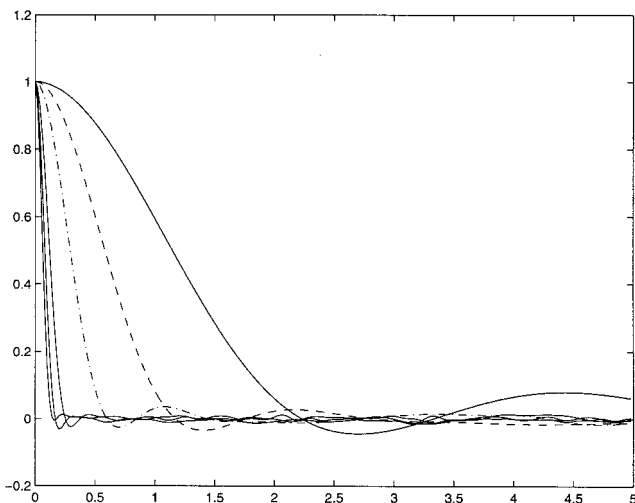

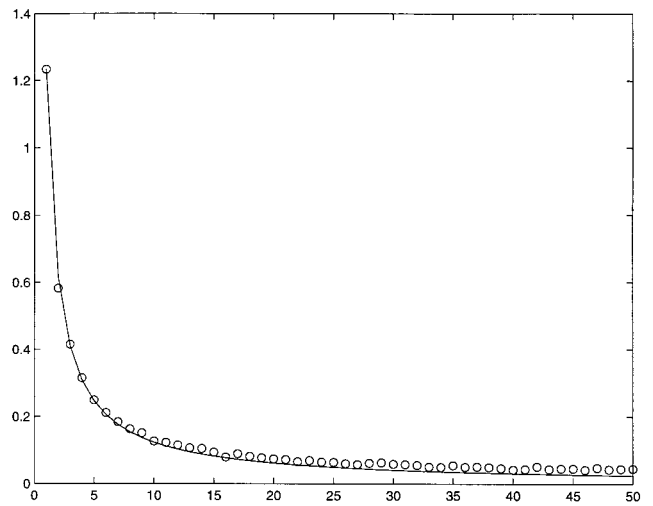**Fig. 4.** Correlation functions for modes $k = 1, 2, 3, 10, 15, 20$.

times in Fig. 5. There, the scaling formula in Eq. **11** is multiplied by a constant to exactly match the correlation time for $k = 1$. As shown in Fig. 5, the simple theory proposed in Eq. **11** is an excellent fit for the large-scale wave numbers k, with $k \leq 15$, which exhibit the largest range of scaling behavior for temporal correlations.

Robustness and Sensitivity of Results

A wide range of simulations of Eq. **5** have been performed by picking random initial data with β varying from $\beta = 10, 50, 75$, whereas Λ also ranges over values $\Lambda = 50, 100, 200$. The equipartition of the spectrum and correlation scaling behavior predicted by the theory in Eqs. **9, 10**, and **11** is very robust, with similar behavior as depicted in Figs. 4 and 5. The only caveat in this discussion is the preconstant for the correlation scaling theory in Eq. **11**, which depends on the correlation time of the largest-scale mode with $k = 1$. This correlation time is a weakly dependent function of Λ; however, the ratio of the largest to the smallest correlation time in the system is independent of Λ for all the parameter regimes tested. Details are presented elsewhere (13).

The statistical predictions of Eq. **9** go beyond the energy spectrum and also predict Gaussian behavior for higher moments. For a Gaussian distribution, fourth moments are equal to three times the square of second moments, whereas sixth moments are equal to fifteen times the cube of second moments. In Fig. 6, the relative error in the Gaussian approximation of fourth and sixth moments from Eq. **9** is computed as a function of wave number from the simulations of Eq. **5** with $\beta = 50$ and $\Lambda = 200$; the larger value of Λ is utilized to avoid dynamic range effects (dividing by small numbers) in processing the numerical output. Fig. 6 *Upper* gives the relative error in the fourth moment prediction; these errors are less than 1% for almost all wave numbers and never exceed 3%, with the largest errors in the low wave number regime. For the sixth moments, the relative errors are less than 2% for most of the wave numbers and do not exceed 6% overall. Thus, further statistical details of the prediction from Eq. **9** are confirmed with surprising accuracy.

Concluding Discussion

In the previous paragraphs, we have introduced a simple model for one-dimensional dynamics that is a suitable approximation of the Burgers–Hopf equation in Eq. **1** involving the Galerkin projection on Fourier modes defined in Eqs. **3** or **5**. Unlike the
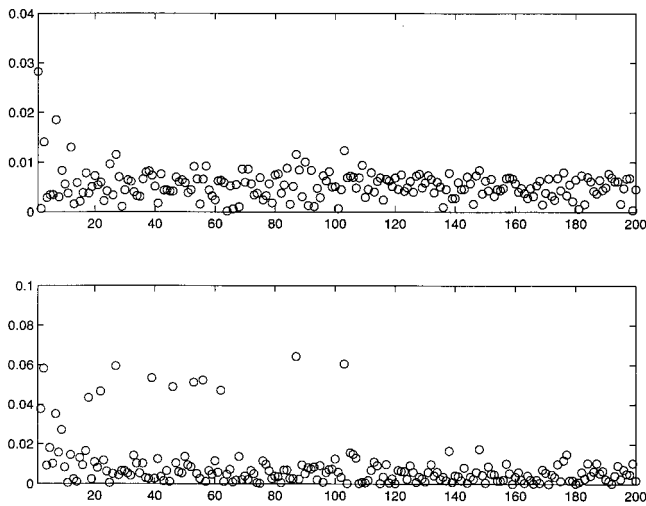
Fig. 6. Relative errors between fourth and sixth moments and appropriate formulas with second moments.

celebrated dissipative and dispersive approximations to Eq. **1**, which exhibit exactly solvable and/or completely integrable behavior, the numerical evidence presented here indicates strong intrinsic chaos with ergodic behavior in the model. Furthermore, the mathematical structure of the model, including conservation of momentum, energy, and the Liouville property, allows for simple statistical predictions for the model that are strongly confirmed by numerical experiments. The model exhibits intrinsic slower decay of temporal correlations at larger scales and the increased predictability of the larger-scale motions in a simple model with intrinsic chaos. This is one of the main achievements of the present paper. Furthermore, simple scaling theories for the behavior of the correlations have been developed, and these predictions are also supported and confirmed by the numerical evidence reported here.

Several intriguing issues regarding the model are worth pursuing in the future. Eq. **1** also conserves the higher invariants, $\int |u|^p$. Thus, are there suitable approximations to Eq. **1** that conserve momentum, energy, and a discrete version of at least one of the higher invariants and also have the Liouville property with a well-defined statistical theory? Another simple issue is whether there are other discrete approximations to Eq. **1** that conserve discrete forms of momentum and energy and also have the Liouville property. We have found a very simple finite difference approximation to Eq. **1** with all of these properties, and the difference scheme used by Zabusky and Kruskal (14) is a second example with these properties. Is the large-scale correlation scaling behavior universal in these systems, as compared with the spectral Galerkin truncation utilized in the model presented here? We discuss all of these issues elsewhere (14).

The original motivation of the "toy" model developed here is to utilize this model to check reduced stochastic modeling procedures for more complex physical or biological models with a range of correlations on a simple unambiguous one-dimensional model system that exhibits such behavior. Cai, Vanden Eijnden, and A.M. have done this for the model and report on this work elsewhere (15).

Spectrally truncated approximation for idealized geophysical flows that conserve both energy and enstrophy play an important role in building idealized climate models (16, 17) where various facets of observational as well as computational (18) and stochastic (ref. 6; A.M., I.T. & E. Vanden Eijnden, unpublished work) modeling phenomena can be checked in a relatively unambiguous context. The even simpler one-dimensional models proposed here have the potential to provide more mathematical insight on a variety of the issues encountered in these problems.

1. Kleeman, R. & Moore, A. (1997) *J. Atmos. Sci.* **54,** 753–767.
2. Saravanan, R. & McWilliams, J. (1997) *J. Climate* **10,** 1114–1127.
3. Branstator, G. (1995) *J. Atmos. Sci.* **52,** 207–226.
4. Schutte, Ch., Fisher, A., Huisinga, W. & Deuflhard, P. (1999) *J. Comp. Phys.* **151,** 146–168.
5. Gordon, H. & Somoraj, R. (1992) *Proteins Struct. Funct. Genet.* **14,** 249–262.
6. Majda, A., Timofeyev, I. & Vanden Eijnden, E. (1999) *Proc. Natl. Acad. Sci. USA* **96,** 14687–14691.
7. Whitham, G. B. (1974) *Linear and Nonlinear Waves* (Academic, New York).
8. Burgers, J. M. (1948) *Adv. Appl. Mech.* **1,** 171–199.
9. Hopf, E. (1950) *Comm. Pure Appl. Math.* **3,** 201–230.
10. Gardener, C. S., Greene, J. M., Kruskal, M. D. & Miura, R. M. (1967) *Phys. Rev. Lett.* **19,** 1095–1097.
11. Goodman, J. & Lax, P. D. (1988) *Comm. Pure Appl. Math.* **41,** 591–613.
12. Pedlosky, J. (1982) *Geophysical Fluid Dynamics* (Springer, New York), 532–535.
13. Majda, A. & Timofeyev, I. (2000) Statistical Mechanics for Truncations of the Burgers–Hopf Equation: A Model for Intrinsic Stochastic Behavior with Scaling, preprint.
14. Zabusky, N. & Kruskal, M. D. (1988) *Phys. Rev. Lett.* **15,** 240–243.
15. Cai, D., Majda, A. & Vanden Eijnden, E. (2000) Stochastic Modeling of Nonlinear Dynamics with Intrinsic Stochasticity and Scaling Behavior, preprint.
16. Leith, C. E. (1975) *J. Atmos. Sci.* **32,** 2022–2025.
17. Carnevale, G. & Frederiksen, J. (1987) *J. Fluid Mech.* **175,** 157–181.
18. Frederiksen, J., Dix, M. & Kepert, S. (1996) *J. Atmos. Sci.* **53,** 887–1004.

APPLIED PHYSICAL SCIENCES